Appl Petrochem Res (2014) 4:297–304
DOI 10.1007/s13203-014-0065-y

ORIGINAL ARTICLE

Hydrogenolysis of bioglycerol to 1,2-propanediol over Ru/CeO_2 catalysts: influence of CeO_2 characteristics on catalytic performance

Gangadhara Raju · Damma Devaiah · Padigapati S. Reddy · Komateedi N. Rao · Benjaram M. Reddy

Received: 13 February 2014 / Accepted: 9 June 2014 / Published online: 2 July 2014

Abstract Hydrogenolysis of glycerol to 1,2-propanediol is an alternative route for efficient utilization of biomass-derived glycerol to value-added chemicals. In this study, catalytic hydrogenolysis of glycerol was systematically investigated over various Ru/CeO_2 catalysts. CeO_2-support was prepared by different methods and Ru deposition by wet impregnation method. Synthesized catalysts were characterized by various techniques, namely, XRD, XPS, TPR, TPD, and other. Hydrothermally synthesized CeO_2-supported Ru catalyst showed relatively more number of acid sites with mild acid strength and exhibited highest conversion and product selectivity. Effect of various parameters including Ru loading, reaction temperature, and hydrogen pressure was evaluated and addressed.

Keywords Glycerol · Hydrogenolysis · Ru/CeO_2 · 1,2-Propanediol · Hydrothermal · Support

Introduction

Production of fuels and chemicals from biomass has attracted much attention recently owing to declining petroleum reserves and increasing concern about global warming [1–3]. The biomass-derived feedstock, bioglycerol, has been identified as one of the top 12 building-block chemicals of biorefinery processes [4]. It is also a promising alternative to petroleum and natural gas for the production of commodity chemicals and materials [4]. Glycerol is formed (about 10 wt%) as a byproduct during biodiesel production by transesterification of vegetable oils or animal fats. The rapid growth of biodiesel industry is expected to facilitate surplus of glycerol in the world market and the price of glycerol is anticipated to decline significantly from the present cost [3, 5, 6]. Therefore, various research groups and industries are working on efficient utilization of glycerol, which makes the biodiesel industry economically more attractive.

A significant research effort has been made recently on the conversion of bioglycerol to various value-added chemicals [3, 5, 7–9]. Synthesis of 1,2-propanediol (1,2-PDO) from glycerol via catalytic hydrogenolysis has attracted much attention, which finds use in the manufacture of unsaturated polyester resins, functional fluids, pharmaceuticals, cosmetics, paints, and foods [10, 11]. As per the recent literature, supported noble metal-based and transition metal-based (mainly Cu and Ni) catalysts are widely investigated for glycerol hydrogenolysis [10–20]. Among the noble metals, supported Ru-based catalysts have been investigated extensively [13, 16, 17]. Interestingly, addition of solid acid catalysts such as, H_2WO_4, amberlyst, zeolites, and sulfated zirconia to the reaction mixture enhanced the catalytic activity [13, 17, 18]. Among those, the ion exchange resin (amberlyst 15) exhibited excellent catalytic activity [17]. However, the reaction temperature range is limited due to thermal instability of the ion exchange resins [7]. Feng et al. [14] investigated the influence of various supports (TiO_2, SiO_2, NaY, γ-Al_2O_3, and active-carbon) on Ru catalysts and found that the support influences strongly the metal particle

Electronic supplementary material The online version of this article (doi:10.1007/s13203-014-0065-y) contains supplementary material, which is available to authorized users.

G. Raju · D. Devaiah · P. S. Reddy · K. N. Rao · B. M. Reddy (✉)
Inorganic and Physical Chemistry Division, CSIR-Indian Institute of Chemical Technology, Uppal Road, Hyderabad 500 007, India
e-mail: bmreddy@iict.res.in; mreddyb@yahoo.com

size and the catalytic activity. Ma et al. [12, 19, 20] have studied the effect of Re dopant on the catalytic performance of Al_2O_3, carbon, and ZrO_2 supported Ru on the conversion of glycerol and the selectivity to propanediols. Vasiliadou et al. [10] studied the effect of support and metal precursors, and concluded that the support strongly influences the activity of Ru and also the acidity of the catalyst. Activated carbon (AC) supported Ru in the presence of amberlyst resin exhibited about 21.3 % glycerol conversion and 76.7 % 1,2-PDO selectivity at 120 °C and 8 MPa H_2 pressure [18]. These studies clearly suggested that support plays a vital role in the hydrogenolysis of glycerol. Glycerol hydrogenolysis normally proceeds through the dehydration of glycerol to acetol followed by the hydrogenation of the intermediate product to 1,2-PDO. For this, the support plays a key role to perform the former step. Therefore, the presence of metallic surface and acidic function of the support are very important for hydrogenolysis of glycerol. Therefore, we have undertaken the investigation of the effect of preparation method of support on the glycerol hydrogenolysis activity.

Ceria and doped ceria-based materials are identified as worthy catalysts for dehydration of various alcohols [21, 22]. CeO_2 has also been reported to show remarkable performance for synthesis of acetol from glycerol [23]. Further, incorporation of CeO_2 into the Ni/AC catalyst exhibited enhanced promoting effect on the hydrogenolysis of glycerol [15]. It was observed that the catalyst activates the C=O bond through interaction of surface oxygen vacancies, which are formed at the ceria surface upon the reduction treatment. It is known that ceria containing catalysts are very promising for selective hydrogenation of aldehydes [24, 25].

In the present study, an attempt has been made to integrate the synthesis and physicochemical characteristics with the catalytic efficiency of Ru/CeO_2 catalysts for hydrogenolysis of glycerol. As known, the preparation method plays a vital role on the specific surface area, acidity, and dispersion of the catalysts. As mentioned previously, the support plays vital role in glycerol hydrogenolysis. Therefore, the CeO_2-support was prepared by different methods. Various physiochemical techniques were employed to gain information on the physicochemical properties of the materials and correlated with the activity for the title reaction.

Experimental section

Synthesis of catalysts

CeO_2 preparation by hydrothermal method

In this method, 3 g of $Ce(NO_3)_3{\cdot}6H_2O$ (Aldrich, AR grade) and 6.4 g of NaOH were dissolved in double-distilled water separately. Then, the NaOH base solution was added dropwise to the Ce-nitrate salt solution under continuous stirring at room temperature. The obtained purple colloidal solution was transferred into an autoclave and gradually heated to 100 °C and kept at this temperature for 12 h. Thus formed solid was washed several times with plenty of double-distilled water and dried at 110 °C for 12 h. Finally, the sample was calcined at 500 °C for 5 h at a heating rate of 5 °C min^{-1} in static air to get CeO_2 (CHT) [26].

CeO_2 preparation by homogeneous precipitation method

In a typical procedure, $Ce(NO_3)_3{\cdot}6H_2O$ was dissolved in double-distilled water and the resulting clear solution was transferred to round bottom flask. To this solution, an aqueous solution of urea (mole ratio of cerium nitrate to urea = 1:3) as precipitating agent was added with continuous stirring at room temperature. The mixed solution was gradually heated to 90 °C to form a brown gel-like solution. After which the resulting solution was digested at the same temperature for 24 h. The formed solid was filtered off and dried at 110 °C for 12 h. The resulting solid was then calcined at 500 °C for 5 h at a heating rate of 5 °C min^{-1} in the static air to obtain CeO_2 (CU).

CeO_2 preparation by modified precipitation method from ultrahigh dilute solution

More details on this preparation method could be found elsewhere [27]. In this method, $Ce(NO_3)_3{\cdot}6H_2O$ and aqueous ammonia were the precursors for CeO_2 and precipitating agent, respectively. The final sample was calcined at 500 °C for 5 h to obtain the CeO_2 (CN).

Ceria-supported Ru catalysts were prepared by a standard wet impregnation method. The required amount of $RuCl_3$ (Aldrich, AR grade) was dissolved in double-distilled water. To this clear solution, previously prepared fine powder of ceria was added under constant stirring. The excess solvent was evaporated on a hot plate with continuous stirring. The resulting material was dried at 110 °C for 12 h and finally calcined at 500 °C for 5 h at a heating rate of 5 °C min^{-1} in the static air. All ceria-supported Ru catalysts are designated as XRC (X = wt% of Ru, R = Ru and C = CHT, CU and CN) for simplicity.

Characterization of catalysts

Surface area and pore volume of the samples were determined on a TriStar 3000 (Micromeritics Instrument Co., USA) instrument at liquid N_2 temperature. Prior to the measurement, samples were degassed at 300 °C for 3 h to remove residual moisture. The BET specific surface areas

were calculated from adsorption data in the relative pressure (P/P_o) range of 0.04–0.25. The total pore volume was estimated from the amount of adsorbed gas at a relative pressure of 0.99. X-ray diffraction (XRD) patterns of the synthesized catalysts were obtained on a Rigaku diffractometer using Cu Kα radiation ($\lambda = 0.154$ nm) source and a scintillation counter detector. The step size and time per step were fixed at 0.02° and 1 s, respectively, in the range of $5° \leq 2\theta \leq 80°$. NH_3-temperature programmed desorption (NH_3-TPD), and H_2-temperature programmed reduction (H_2-TPR) measurements were carried out by using an AutoChem II 2920 (Micromeritics Instrument Co., USA) instrument [28]. X-ray photoelectron spectroscopy (XPS) analysis was performed on a PHI 5000 Versa Probe (Ulvac-PHI) spectrometer using Al Kα (1,486.6 eV) radiation. The analysis was done at room temperature and the pressure was typically at 6.7×10^{-8} Pa. The charging of samples was corrected by setting the binding energy of the adventitious carbon (C 1 s) at 284.6 eV. The SEM images of the catalysts were recorded on a JEOL-JSM 5600 instrument.

Hydrogenolysis of glycerol

Glycerol hydrogenolysis was carried out in 300-mL stainless steel autoclave (Parr Instruments, USA). In a typical experiment, an aqueous solution of glycerol (20 %) and catalyst (glycerol to catalyst weight ratio = 10:1) were charged in the autoclave. Prior to the catalytic run, the catalyst was activated in hydrogen steam (30 mL min^{-1}) at 200 °C for 2 h. After which the autoclave was purged 4–5 times with H_2 to remove the air in the headspace. The reactor was then heated to the desired reaction temperature and pressurized with hydrogen gas. A constant decrease in the H_2 pressure during the reaction was witnessed due to the consumption of hydrogen. After 12 h of reaction, the reaction mixture was allowed to cool down to room temperature and the separated liquid products from the catalyst were analyzed by gas chromatography using OPTIMA-WAX capillary column (30 m × 0.53 mm × 1 μm) and flame ionization detector. The reaction products were identified by GC–MS (Shimadzu) whenever required. The main products that were analyzed include 1,2-PDO, ethylene glycol, 1-propanol, 2-propanol, methanol and ethanol.

Results and discussions

XRD

XRD patterns of various Ru/CeO_2 samples are depicted in Fig. 1. The diffraction peaks could be indexed to (111), (200), (220), (311), (222), (400), (331), and (420) faces

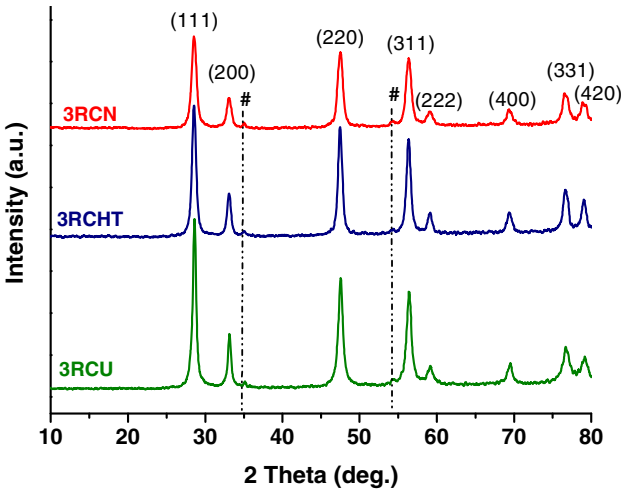

Fig. 1 XRD pattern of various CeO_2-supported Ru samples (*hash symbol* RuO_2)

corresponding to a face-centered cubic fluorite structure of CeO_2 (space group *Fm3m*, PDF-ICDD # 34-0394). The observed small diffraction lines at 35.02° and 54.36° are due to RuO_2 which signifies that the ruthenium oxide particles are in a highly dispersed state on the support. For below 3 wt% of Ru, the XRD peaks corresponding to only ceria were observed (Fig. S1, Supporting Information). The absence of RuO_2 XRD peaks could be either due to a well-dispersed state on the support or the presence of RuO_2 below the detection limit of the XRD technique. The samples with Ru loading ≥3 wt% exhibited the peaks corresponding to both RuO_2 and CeO_2.

BET surface area and pore volume

The BET surface area and pore volume results of various samples are tabulated in Table 1. The surface area of 3RCHT, 3RCU, and 3RCN catalysts is 46, 39, and 33 $m^2\ g^{-1}$, respectively. The ceria support synthesized by hydrothermal (3RCHT) method exhibited a high specific surface area than others. Moreover, a high cumulative pore volume was also noted for 3RCHT sample. It implies that the synthesis method significantly influences the specific surface area and pore volume of the catalysts. The specific surface area and pore volume of the samples were found to decrease upon impregnation with Ru. Deposition of Ru in various amounts from 1 to 7 wt% over the CHT support resulted a decrease in the BET surface area of the catalysts from 49 to 38 $m^2\ g^{-1}$. The decrease in the surface area of the catalysts could be attributed to penetration of the deposited active ruthenium oxide into the pores of the support thereby blocking some of the pores. However, the measured surface area and cumulative pore volume of 3RCHT sample are considerably higher in comparison to 3RCU and 3RCN samples.

Table 1 BET surface areas and pore volumes of various CeO_2-supported Ru samples

Catalyst	BET surface area ($m^2\ g^{-1}$)	Pore volume ($cm^3\ g^{-1}$)
3RCN	33	0.050742
3RCU	39	0.052171
3RCHT	46	0.152042
1RCHT	49	0.159472
5RCHT	42	0.144154
7RCHT	38	0.125671

TPD and TPR studies

To know the acidic properties of the catalysts, the NH_3-TPD experiments were conducted. The NH_3-TPD profiles of 3RCHT, 3RCU, and 3RCN samples are presented in Fig. 2. The characteristic acid strengths of various samples are normally expressed in temperature ranges where NH_3 is desorbed. The NH_3 desorbed below 200 °C is the measure of weak acidic sites. The desorption temperature range between 200 and 350 °C and above 350 °C corresponds to medium and strong acid sites, respectively [28]. All the samples exhibited similar characteristic TPD profiles. The 3RCHT sample exhibited three desorption temperature maximums (T_{max}) located at low- (∼135 and ∼198 °C) and high-temperature (∼380 °C) regions attributed to weak and medium strength acid sites, respectively. However, for 3RCN sample the T_{max} was observed at ∼153, ∼254, and ∼415 °C due to weak, medium, and strong acid sites, respectively. The deconvoluted NH_3-TPD profiles and percentage distribution of acid sites (after deconvolution) of various CeO_2-supported Ru samples are presented in Figure S4 and Table S1 (Supporting Information), respectively. As mentioned, the desorption temperature is normally related to the strength of the acid sites. The T_{max} of 3RCHT sample is observed at lower temperatures than other samples. It implies that the acid strength of 3RCHT sample is relatively low. Interestingly, for all samples, more number of acid sites are located at weak acid sites region. The 3RCHT and 3RCU samples exhibited more number of acid sites (large peak area) than 3RCN. These results indicate that synthesis method of CeO_2 is significantly influencing the strength and number of acid sites of the catalysts.

The H_2-TPR profiles of various CeO_2-supported Ru samples are shown in Fig. 3. For all samples, two H_2 consumption peaks were observed. The TPR profile of 3RCN sample exhibited an intense peak at low-temperature region and a very small broad peak at high-temperature region. Unlike 3RCN, the 3RCHT sample exhibited an intense peak at high-temperature region and a low intense peak at low-temperature region. The second reduction

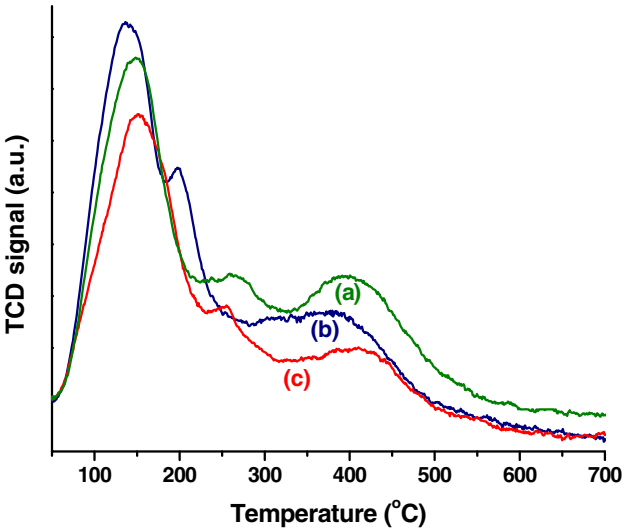

Fig. 2 NH_3-TPD profiles of *a* 3RCU, *b* 3RCHT and *c* 3RCN samples

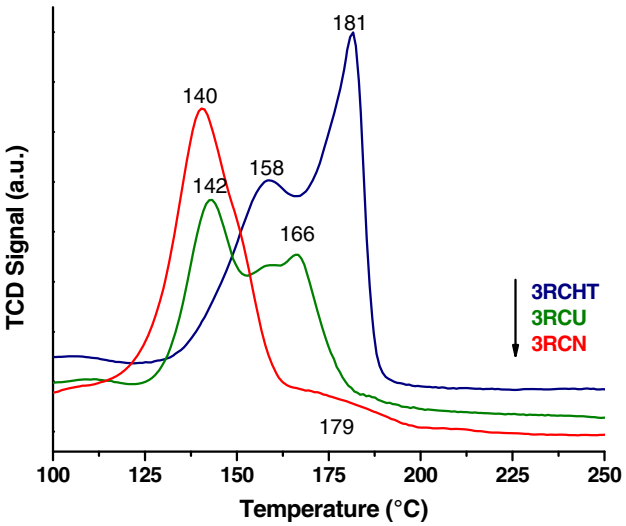

Fig. 3 TPR profiles of various CeO_2-supported Ru samples

temperature peak was also reported for Ru/TiO_2 and Ru/Al_2O_3 catalysts at 185 and 340 °C, respectively [29, 30]. This peak is usually attributed to the reduction of Ru_2O_3 particles that are strongly interacting with the support and are thus more difficult to reduce to metallic Ru [29, 30]. However, the diffraction peaks pertaining to Ru_2O_3 phase are not found in the XRD profiles (Fig. 1). Triki et al. [31] also reported a similar reduction profile centered at 220 °C with a shoulder at 175 °C for Ru/Ce–Al catalyst and assigned them to the reduction of Ru-oxide interacting with CeO_2 and free or dispersive nature of Ru-oxide, respectively. Interestingly, both H_2 consumption peaks were shifted to high-temperature side for 3RCHT sample compared to other samples. These results obviously envisage that there is a strong interaction between Ru-oxide and ceria support in the 3RCHT catalyst. Notably, for all

samples, the reduction temperature of Ru-oxide is lower than the activation temperature employed (prior to reaction, catalysts were activated in H_2 at 200 °C).

XPS measurements

XPS was employed to investigate the surface structure and oxidation states of the catalysts. The XP spectra of Ce 3d core level for various samples are presented in Figure S2 (Supporting Information). The XPS main bands labeled u_0 and u with satellite bands u', u'', and u''' are ascribed to the Ce $3d_{3/2}$ ionization, respectively. The main bands related to Ce $3d_{5/2}$ ionization are labeled as v and v_0 with satellite bands v', v'', and v''', respectively. The main bands u/v and shakedown doublet u''/v'' are the features corresponding to Ce $3d^9$ $4f^2$ O $2p^4$ and Ce $3d^9$ $4f^1$ O $2p^5$ final states. The highest binding energy u''' and v''' bands are the result of a Ce $3d^9$ $4f^0$ O $2p^6$ final state. These doublets are corresponding to the pairs of spin–orbit doublets characteristic of the presence of tetravalent Ce ions (Ce^{4+}) in the sample. The lowest binding energy u_0 and v_0 bands located at ~899.5 and ~880.9 eV, respectively, are the result of Ce $3d^9$ $4f^2$ O $2p^5$ final state. Similarly, the satellite bands u'/v' are assigned to final state of Ce(III) $3d^9$ $4f^1$ O $2p^6$. The u'/v' and u_0/v_0 doublets are due to photoemission from Ce^{3+} cations. These results clearly reveal that the synthesized ceria support is in mixed 4+ and 3+ valent state [27, 32, 33]. Interestingly, the peaks of Ce 3d XP spectra of 3RCHT sample are slightly shifted to lower binding energy side in comparison to other samples.

The XP spectra of Ru 3d core level for various samples are presented in Fig. 4. In the region of Ru, two peaks related to Ru $3d_{5/2}$ and Ru $3d_{3/2}$ transitions are found. As shown in the figure, the Ru cation in various samples exhibited peaks at 281.2 and 280.7 eV corresponding to Ru $3d_{5/2,}$ respectively. The band at 280.7 eV for 3RCU and 3RCN samples is ascribed to Ru^{4+} (RuO_2). The Ru ($3d_{5/2}$)-binding energy of the 3RCHT sample is slightly higher than the binding energy of the bulk RuO_2 (280.4–281.0 eV) and lower than the binding energy of RuO_3 (282.5 eV) [34]. However, agrees well with the binding energy of Ru^{4+} ($3d_{5/2}$) in $Ce_{0.95}Ru_{0.05}O_{2-\delta}$ and $RuO_2{\cdot}xH_2O$ [34]. The shift toward higher binding energy side is probably due to strong interaction between Ru- and Ce-oxides [35]. Interestingly, in the Ce 3d XP spectra of 3RCHT sample (Fig. S2, Supporting Information) the binding energy values are shifted to lower binding energy side when compared to 3RCU and 3RCN samples. Therefore, XP spectra of both Ce and Ru 3d clearly reveal that Ru- and Ce-oxides are strongly interacting in the 3RCHT sample compared to 3RCN and 3RCU samples. The shift in the Ru-oxide reduction peak in the TPR to high-temperature side (Fig. 3) has also confirmed the same.

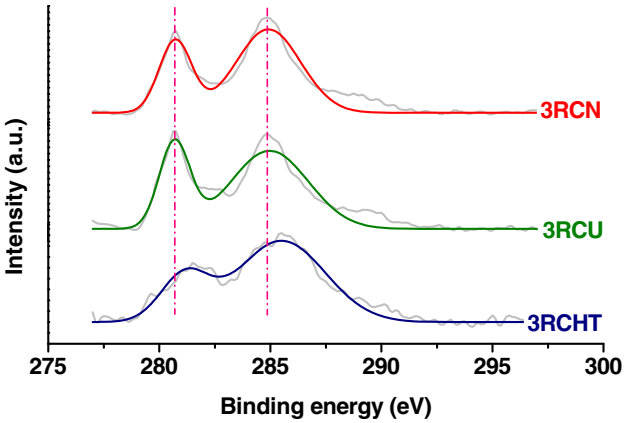

Fig. 4 Ru 3d XP spectra of various CeO_2-supported Ru samples

Another peak at around 285 eV assigned to Ru $3d_{3/2}$ is considered to contain the C 1 s component. The characterization results clearly reveal that synthesis method of CeO_2 influences the surface properties of the catalysts. The surface morphologies of catalysts as revealed by SEM images also confirm the effect of preparation method (Fig. S3, Supporting Information).

Catalytic activity measurements

Influence of CeO_2 preparation method

Hydrogenolysis of glycerol was carried out over various CeO_2-supported Ru catalysts. The influence of CeO_2 preparation method on glycerol conversion and 1,2-PDO selectivity are shown in Table 2. The bare CeO_2-support exhibited very poor catalytic activity (glycerol conversion below 1 %, details are not shown here) under the reaction conditions employed. Interestingly, the Ru/CeO_2 samples exhibited superior catalytic activity (Table 2) under the same reaction conditions. This clearly envisages the significance of both acidic and metal sites for this reaction. Kusunoki et al. [17] also observed an enhanced hydrogenolysis activity due to strong synergy between the metal and the acid function of the catalyst by the addition of acid additives to Ru/C catalyst. The 3RCHT sample exhibited a high glycerol conversion (72.7 %) with 66 % selectivity of 1,2-PDO. On the other hand, the conversion of glycerol was 47.2 and 36.2 % over 3RCU and 3RCN samples, respectively. A more pronounced influence was observed in the case of CeO_2-support synthesized by hydrothermal method (3RCHT), on which the activity was found to increase significantly. The Table 2 clearly reveals that the preparation method of support strongly influences the performance of the catalysts. The essential feature of an excellent hydrogenolysis catalyst is that it should promote the dehydration of glycerol to an intermediate product,

Table 2 Glycerol hydrogenolysis over various CeO_2-supported Ru catalysts

Catalyst	Glycerol conversion (%)	Selectivity (%)			Yield (1,2-PDO)
		1,2-PDO	Ethylene glycol	Others[a]	
3RCHT	72.7	66.0	5.2	28.8	47.9
3RCU	47.2	77.2	8.2	14.6	36.4
3RCN	36.2	69.4	7.6	23.0	25.1

Reaction conditions: 50 mL of 20 % aqueous glycerol solution, 6 MPa pressure, 1 g catalyst, 200 °C reaction temperature and 12 h reaction time

[a] Others = 1-propanol, 2-propanol, methanol and ethanol

acetol, and subsequent hydrogenation of the acetol to the desired product, 1,2-PDO. In addition to this, the catalyst should be able to suppress the consecutive hydrogenolysis of 1,2-PDO and degradation reactions. The 3RCU catalyst exhibited a high selectivity of 1,2-PDO (77.2 %) compared to other samples. However, the 3RCHT catalyst exhibited a high glycerol conversion. Further, the selectivity of ethylene glycol is much lower in the case of 3RCHT sample than others. It implies that the 3RCHT sample inhibited the C–C bond cleavage to form ethylene glycol than others. Interestingly, the NH_3-TPD results demonstrated that the acid strength of 3RCHT and 3RCU samples is lower than the 3RCN. The acid strength of various samples is in the following order: 3RCHT < 3RCU < 3RCN. In contract to this the yield of 1,2-PDO over various samples is as follows: 3RCHT > 3RCU > 3RCN. In addition, the total acidity as determined by NH_3-TPD is also more for 3RCHT and 3RCU samples than 3RCN. It has been well established in the literature that hydrogenolysis over supported noble metal catalysts is strongly influenced by the acidity of the support material [10]. Recently, Lee and Moon [36] also reported that the acidity of catalyst enhances when both Ca and Zn were added to Ru–Mg/Al catalyst which results in increased glycerol conversion and selectivity. These results clearly indicate that the acid strength and total acidity are the significant factors in the determination of hydrogenolysis activity and selectivity, because acid sites promote the initial step of the hydrogenolysis of glycerol, i.e., dehydration of glycerol to acetol. In addition, the TPR and XPS analysis revealed that the Ru-oxide is strongly interacting with the support in the case 3RCHT sample than others. Moreover, the 3RCHT sample also exhibited a high specific surface area compared to other samples. High surface area obviously exhibits better catalytic activity, because a large specific surface area provides more active sites for adsorbing the reactants. From these results, one can speculate that the hydrogenolysis activity of Ru/CeO_2 is strongly dependent on the specific surface area, acid strength, total acidity, and metal–support interaction.

Table 3 Effect of Ru content on glycerol hydrogenolysis

Ru (wt%)	Glycerol conversion (%)	Selectivity (%)			Yield (1,2-PDO)
		1,2-PDO	Ethylene glycol	Others[a]	
1	45.7	70.1	6.3	23.6	32.0
3	72.7	66.0	5.2	28.8	47.9
5	100	53.2	3.2	43.6	53.2
7	100	40.2	0.9	58.9	40.2

Support CHT, Ru = 1–7 wt%, reaction conditions same as Table 2

[a] Others = 1-propanol, 2-propanol, methanol and ethanol

Further, the influence of these factors on the hydrogenolysis activity is highly interdependent.

Influence of Ru loading

A series of catalysts with different Ru contents (1, 3, 5, and 7 wt%) were prepared to investigate the effect of Ru loading on glycerol hydrogenolysis and the results are depicted in Table 3. Interestingly, the glycerol conversion increased with increase in Ru metal content and reached a maximum conversion (100 %). These results infer that Ru is also responsible for the dehydration of glycerol to acetol, the intermediate product, which on further hydrogenation leads to the formation of 1,2-PDO. Chiu et al. [37] investigated the dehydration of glycerol over transition metal catalysts with reactive distillation technology and the formed acetol was successfully isolated. The selectivity of 1,2-PDO and ethylene glycol was observed to decline with a rise in the Ru content. The decrease in the selectivity of 1,2-PDO is found to be due to further hydrogenolysis of 1,2-PDO to lower alcohols. However, a maximum yield of 1,2-PDO (54.2) was obtained at 5 wt% Ru on the CeO_2.

Influence of reaction temperature

Glycerol hydrogenolysis was performed at various temperatures from 180 to 220 °C at 6 MPa in the presence of 3RCHT catalyst, and the results are presented in Table S2 (Supporting Information). As observed from this figure, the reaction temperature has a significant effect on the catalytic performance of various samples. As the reaction temperature increases from 180 to 220 °C, there is a uniform increase in the glycerol conversion. At 180 °C, the glycerol conversion was only 22.7 % and reached to 100 % at 220 °C. However, at high reaction temperatures, the selectivity of 1,2-PDO declined from 65 to 57.7 % corresponding to an increase in the selectivity of ethylene glycol. This observation indicates that a high reaction temperature favors the formation of degradation products due to C–C bond cleavage. However, the overall yield of 1,2-PDO also enhanced with the temperature.

Influence of H_2 pressure

Further, the effect of hydrogen pressure on the glycerol hydrogenolysis was also investigated over 3RCHT catalyst at different pressures from 4 to 8 MPa at a constant temperature of 200 °C. The glycerol conversion and product distribution are presented in Table S3 (Supporting Information). Glycerol conversion increased from 18 to 83.9 % as the H_2 pressure increases from 4 to 8 MPa. The yield of 1,2-PDO also gradually enhanced with increase in the reaction pressure. It implies that hydrogen pressure has a positive effect on the hydrogenolysis of glycerol. The concentration of hydrogen increases in the liquid phase with increase in hydrogen pressure and would drive the reaction equilibrium toward 1,2-PDO formation.

Conclusions

Glycerol hydrogenolysis was investigated over various Ru/CeO_2 catalysts. The CeO_2-support was prepared by different methods to study the influence of synthesis method on glycerol hydrogenolysis activity. The preparation method of the support has a significant effect on the morphology, structural, and textural properties of the catalysts, and also on the hydrogenolysis activity. Among the investigated catalysts, Ru supported on CeO_2 synthesized by hydrothermal method (3RCHT) exhibited high catalytic activity with a glycerol conversion and 1,2-PDO selectivity of 72.4 and 66 %, respectively. The characterization results revealed that the 3RCHT sample exhibits more acid sites with lower acid strength. There is a strong interaction between Ru- and Ce-oxides. Further, a high specific surface area and pore volume were observed in the case of 3RCHT sample. These characteristics were found to show a profound influence on the catalytic activity and selectivity. The catalyst composition, reaction temperature, and pressure were found to influence significantly on the activity and selectivity.

Acknowledgments G.R., D.D., and P.S.R. thank Council of Scientific and Industrial Research (CSIR), New Delhi, for the award of Senior Research Fellowships. The authors thank CSIR, New Delhi for financial support of this work under NMITLI program (TLP-0014).

References

1. Sheldon RA (2011) Utilisation of biomass for sustainable fuels and chemicals: molecules, methods and metrics. Catal Today 167(1):3–13. doi:10.1016/j.cattod.2010.10.100
2. Corma A, Iborra S, Velty A (2007) Chemical routes for the transformation of biomass into chemicals. Chem Rev 107(6):2411–2502. doi:10.1021/cr050989d
3. Jerome F, Pouilloux Y, Barrault J (2008) Rational design of solid catalysts for the selective use of glycerol as a natural organic building block. ChemSusChem 1:586–613. doi:10.1002/cssc.200800069
4. Werpy T, Petersen G (2004) US DOE report: top value added chemicals from biomass, vol 1: results of screening for potential candidates from sugars and synthesis gas. https://www1.eere.energy.gov/bioenergy/pdfs/35523.pdf
5. Zhou CH, Beltramini JN, Fan YX, Lu GQ (2008) Chemoselective catalytic conversion of glycerol as a biorenewable source to valuable commodity chemicals. Chem Soc Rev 37:527–549. doi:10.1039/B707343G
6. Behr A, Eilting J, Irawadi K, Leschinski J, Lindner F (2008) Improved utilization of renewable resources: new important derivatives of glycerol. Green Chem 10:13–30. doi:10.1039/B710561D
7. Reddy PS, Sudarsanam P, Raju G, Reddy BM (2010) Synthesis of bio-additives: acetylation of glycerol over zirconia-based solid acid catalysts. Catal Commun 11(15):1224–1228. doi:10.1016/j.catcom.2010.07.006
8. Reddy PS, Sudarsanam P, Raju G, Reddy BM (2012) Selective acetylation of glycerol over CeO_2–M and SO_4^{2-}/CeO_2–M (M = ZrO_2 and Al_2O_3) catalysts for synthesis of bioadditives. J Ind Eng Chem 18(2):648–654. doi:10.1016/j.jiec.2011.11.063
9. Reddy PS, Sudarsanam P, Mallesham B, Raju G, Reddy BM (2011) Acetalisation of glycerol with acetone over zirconia and promoted zirconia catalysts under mild reaction conditions. J Ind Eng Chem 17(3):377–381. doi:10.1016/j.jiec.2011.05.008
10. Vasiliadou ES, Heracleous E, Vasalos IA, Lemonidou AA (2009) Ru-based catalysts for glycerol hydrogenolysis—effect of support and metal precursor. Appl Catal B Environ 92(1–2):90–99. doi:10.1016/j.apcatb.2009.07.018
11. Dasari MA, Kiatsimkul P–P, Sutterlin WR, Suppes GJ (2005) Low-pressure hydrogenolysis of glycerol to propylene glycol. Appl Catal A Gen 281(1–2):225–231. doi:10.1016/j.apcata.2004.11.033
12. Ma L, He D (2010) Influence of catalyst pretreatment on catalytic properties and performances of Ru–Re/SiO_2 in glycerol hydrogenolysis to propanediols. Catal Today 149(1–2):148–156. doi:10.1016/j.cattod.2009.03.015
13. Furikado I, Miyazawa T, Koso S, Shimao A, Kunimori K, Tomishige K (2007) Catalytic performance of Rh/SiO_2 in glycerol reaction under hydrogen. Green Chem 9:582–588. doi:10.1039/B614253B
14. Feng J, Fu H, Wang J, Li R, Chen H, Li X (2008) Hydrogenolysis of glycerol to glycols over ruthenium catalysts: effect of support and catalyst reduction temperature. Catal Commun 9(6):1458–1464. doi:10.1016/j.catcom.2007.12.011
15. Yu W, Zhao J, Ma H, Miao H, Song Q, Xu J (2010) Aqueous hydrogenolysis of glycerol over Ni–Ce/AC catalyst: promoting effect of Ce on catalytic performance. Appl Catal A Gen 383(1–2):73–78. doi:10.1016/j.apcata.2010.05.023
16. Miyazawa T, Kusunoki Y, Kunimori K, Tomishige K (2006) Glycerol conversion in the aqueous solution under hydrogen over Ru/C^+ an ion-exchange resin and its reaction mechanism. J Catal 240(2):213–221. doi:10.1016/j.jcat.2006.03.023
17. Kusunoki Y, Miyazawa T, Kunimori K, Tomishige K (2005) Highly active metal–acid bifunctional catalyst system for hydrogenolysis of glycerol under mild reaction conditions. Catal Commun 6(10):645–649. doi:10.1016/j.catcom.2005.06.006
18. Miyazawa T, Koso S, Kunimori K, Tomishige K (2007) Development of a Ru/C catalyst for glycerol hydrogenolysis in combination with an ion-exchange resin. Appl Catal A Gen 318:244–251. doi:10.1016/j.apcata.2006.11.006

19. Ma L, He D (2009) Hydrogenolysis of glycerol to propanediols over highly active Ru–Re bimetallic catalysts. Top Catal 52(6–7):834–844. doi:10.1007/s11244-009-9231-3
20. Ma L, He D, Li Z (2008) Promoting effect of rhenium on catalytic performance of Ru catalysts in hydrogenolysis of glycerol to propanediol. Catal Commun 9(15):2489–2495. doi:10.1016/j.catcom.2008.07.009
21. Sato S, Takahashi R, Sodesawa T, Honda N, Shimizu H (2003) Selective dehydration of diols to allylic alcohols catalyzed by ceria. Catal Commun 4(2):77–81. doi:10.1016/S1566-7367(02)00260-1
22. Reddy BM, Thrimurthulu G, Saikia P, Bharali P (2007) Silica supported ceria and ceria–zirconia nanocomposite oxides for selective dehydration of 4-methylpentan-2-ol. J Mol Catal A: Chem 275(1–2):167–173. doi:10.1016/j.molcata.2007.05.037
23. Kinage AK, Upare PP, Kasinathan P, Hwang YK, Chang J-S (2010) Selective conversion of glycerol to acetol over sodium-doped metal oxide catalysts. Catal Commun 11(7):620–623. doi:10.1016/j.catcom.2010.01.008
24. Li H, Zhang S, Luo H (2004) A Ce-promoted Ni–B amorphous alloy catalyst (Ni–Ce–B) for liquid-phase furfural hydrogenation to furfural alcohol. Mater Lett 58(22–23):2741–2746. doi:10.1016/j.matlet.2004.04.003
25. Reddy BM, Rao KN, Reddy GK (2009) Controlled hydrogenation of acetophenone over Pt/CeO_2–MO_x (M = Si, Ti, Al, and Zr) catalysts. Catal Lett 131(1–2):328–336. doi:10.1007/s10562-009-9945-7
26. Tana, Zhang M, Li J, Li H, Li Y, Shen W (2009) Morphology-dependent redox and catalytic properties of CeO_2 nanostructures: nanowires, nanorods and nanoparticles. Catal Today 148(1–2):179–183. doi:10.1016/j.cattod.2009.02.016
27. Reddy BM, Katta L, Thrimurthulu G (2010) Novel nanocrystalline $Ce_{1-x}La_xO_{2-\delta}$ ($x = 0.2$) solid solutions: structural characteristics and catalytic performance. Chem Mater 22(2):467–475. doi:10.1021/cm903282w
28. Raju G, Reddy BM, Abhishek B, Mo Y-H, Park S-E (2012) Synthesis of C4 olefins from *n*-butane over a novel VO_x/SnO_2–ZrO_2 catalyst using CO_2 as soft oxidant. Appl Catal A Gen 423–424:168–175. doi:10.1016/j.apcata.2012.02.040
29. Perkas N, Teo J, Shen S, Wang Z, Highfield J, Zhong Z, Gedanken A (2011) Supported Ru catalysts prepared by two sonication-assisted methods for preferential oxidation of CO in H_2. Phys Chem Chem Phys 13:15690–15698. doi:10.1039/C1CP21870K
30. Fu X, Yu H, Peng F, Wang H, Qian Y (2007) Facile preparation of RuO_2/CNT catalyst by a homogenous oxidation precipitation method and its catalytic performance. Appl Catal A Gen 321(2):190–197. doi:10.1016/j.apcata.2007.02.002
31. Triki M, Ksibi Z, Ghorbel A, Medina F (2011) Preparation and characterization of CeO_2–Al_2O_3 aerogels supported ruthenium for catalytic wet air oxidation of *p*-hydroxybenzoic acid. J Sol-Gel Sci Technol 59(1):1–6. doi:10.1007/s10971-011-2452-5
32. Reddy BM, Thrimurthulu G, Katta L, Yamada Y, Park S-E (2009) Structural characteristics and catalytic activity of nanocrystalline ceria–praseodymia solid solutions. J Phys Chem C 113(36):15882–15890. doi:10.1021/jp903644y
33. Beche E, Charvin P, Perarnau D, Abanades S, Flamant G (2008) Ce 3d XPS investigation of cerium oxides and mixed cerium oxide ($Ce_xTi_yO_z$). Surf Interface Anal 40(3–4):264–267. doi:10.1002/sia.2686
34. Singh P, Mahadevaiah N, Parida SK, Hegde MS (2011) Ru^{4+} ion in CeO_2 ($Ce_{0.95}Ru_{0.05}O_{2-\delta}$): a non-deactivating, non-platinum catalyst for water gas shift reaction. J Chem Sci 123(5):577–592. doi:10.1007/s12039-011-0118-z
35. Sun Z, Wang X, Liu Z, Zhang H, Yu P, Mao L (2010) Pt–Ru/CeO_2/carbon nanotube nanocomposites: an efficient electrocatalyst for direct methanol fuel cells. Langmuir 26(14):12383–12389. doi:10.1021/la101060s
36. Lee S-H, Moon DJ (2011) Studies on the conversion of glycerol to 1,2-propanediol over Ru- based catalyst under mild conditions. Catal Today 174(1):10–16. doi:10.1016/j.cattod.2011.03.071
37. Chiu C-W, Dasari MA, Suppes GJ, Sutterlin WR (2006) Dehydration of glycerol to acetol via catalytic reactive distillation. AIChE J 52:3543–3548. doi:10.1002/aic.10951